IMPROVEMENT OF MC SI SOLAR CELLS BY AL-GETTERING AND HYDROGEN PASSIVATION

G. Hahn, W. Jooss, M. Spiegel, P. Fath, G. Willeke, E. Bucher,
University of Konstanz, Faculty of Physics, P.O. Box X916, D-78457 Konstanz, Germany

ABSTRACT

Systematic Al-gettering and MIRHP (Microwave Induced Remote Hydrogen Plasma) passivation studies have been carried out on various ribbon (EFG, Bayer RGS) and multicrystalline (mc) Si materials (Baysix, Eurosil, Solarex, EMC) with initial minority carrier diffusion lengths varying from <30-300 µm. Gettering was investigated between 700-1050° C. Solar cells with optimized Al-gettering conditions including a selective emitter structure were characterized before and after MIRHP passivation in order to separate the benefits of gettering and hydrogen passivation. We could achieve improvements for most materials by Al-gettering and an increase in all cell parameters for all materials by MIRHP passivation, with an increase in efficiency for the ribbon Si materials of up to 30% relative.

INTRODUCTION

At present the largest part of the solar cell production is based on cast mc Si. This is due to higher costs and the shortage of monocrystalline Si wafers which show better performance parameters. In the last years a lot of effort was made to improve the quality of mc Si using different techniques such as various gettering processes and hydrogen passivation [1,2]. With the employment of these techniques efficiencies of up to 18.6% could be reached on a 1x1 cm^2 Crystal Systems HEM mc Si solar cell [3]. The next step in reducing the costs for solar cell production could be the use of even cheaper ribbon Si. These materials have in common that no losses due to wafer cutting from large ingots occur, less expense for the wafer production is needed and a high throughput is expected. Because of the even lower Si quality of these materials [4,5] (crystal defects, purity, oxygen content) as compared to cast mc Si the use of the techniques mentioned above is again very important to improve J_{sc}, V_{oc} and thus the cell efficiencies. Ribbon Si solar cell performance is lower than that of cast mc Si in most cases but the cheaper wafer production should overcompensate this disadvantage. Thus ribbon Si is an economically attractive alternative to standard cast Si. This study was carried out in order to find the optimum Al-gettering and hydrogen passivation for ribbon and cast mc Si materials manufactured with different methods.

USED MATERIALS

In our study we have chosen seven mc Si materials from differing manufacturing processes. Baysix, Eurosil P43 and P48 and Solarex are all standard, EMC is an electromagnetically cast mc Si whereas EFG (Edge-defined Film-fed Grown) and Bayer RGS (Ribbon Growth on Substrate) are ribbon Si. Due to the different manufacturing methods the Si materials show large differences in the minority charge carrier diffusion length L_{diff}. In Table 1 the approximate L_{diff} of the source materials before processing as determined by SPV (Surface PhotoVoltage) measurements can be found. As expected L_{diff} shows the lowest values for the ribbon Si materials because of impurities and a high oxygen concentration present especially in RGS [5].

Table 1. Approximate minority charge carrier diffusion length L_{diff} for the materials used in this study before processing as determined by SPV measurements.

Material	approx. L_{diff} by SPV [µm]
Baysix	130
Eurosil P43	120
Eurosil P48	>150
Solarex	<100
EMC	100
EFG	<80
RGS	<30

For our study we used neighboring 5x5 cm^2 wafers with the same crystal grain structure in the case of the cast mc Si in order to be able to compare the four 2x2 cm^2 cells prepared from these wafers after processing. For the selection of EFG material we took neighboring wafers from one EFG tube.

AL-GETTERING STUDY

In the first part of our study we investigated the impact of the Al-gettering temperature on the cell parameters, especially on J_{sc} and V_{oc}. In Fig. 1 the applied solar cell process for the gettering study is shown schematically. A leveling of the ribbon Si with a conventional wafer dicing saw was done to be able to use photolithography. 2 µm of Al were evaporated and a gettering step of 30 min at temperatures between 700-1050° C under N_2 atmosphere was applied. In Fig. 2 Al-gettering results for Eurosil P48

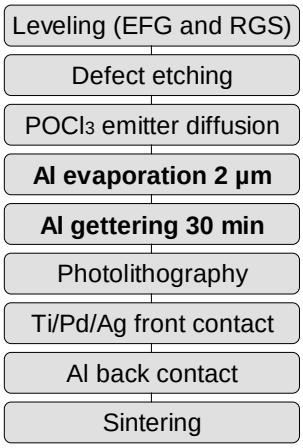

Fig. 1. Process sequence for the Al-gettering study.

are presented. The four different symbols represent the four cells with a different crystal grain structure. We could demonstrate improvements in both J_{sc} and V_{oc} resulting in an optimal Al-gettering temperature of about 900-1000° C.

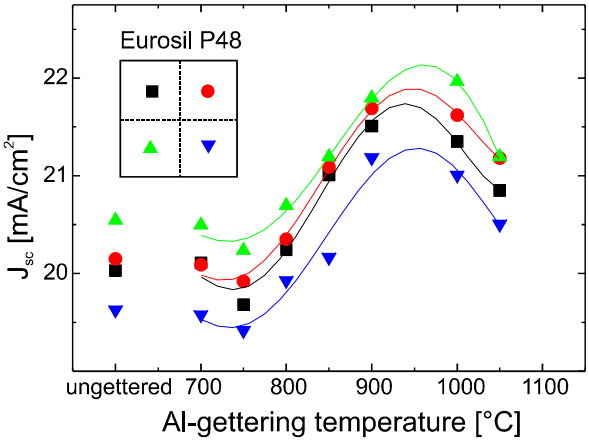

Fig. 2. Al-gettering results for Eurosil P48. The four symbols represent the four 2x2 cm^2 cells from one 5x5 cm^2 wafer with the same grain structure.

In order to prove that the increase in J_{sc} is combined with an increase in L_{diff} we carried out spectral response measurements and fitted the obtained results in the long wavelength region with two dimensional computer simulations as described in [6]. Table 2 shows the results for the ungettered reference cell and the Al-gettered cells with the same grain structure. L_{diff} is increased by 20 µm for a gettering temperature of 950° C which is in agreement with the results of Fig. 2.
Table 3 provides an overview for all materials and their optimum Al-gettering temperature T_{opt}. For Solarex material a decrease in L_{diff} could be observed, whereas Baysix and Eurosil P43 showed nearly identical diffusion lengths with or without an Al-gettering step. In the other materials L_{diff} can be significantly increased by an Al-gettering step at the optimum temperature T_{opt} shown.

Table 2. L_{diff} for ungettered and Al-gettered cells of Eurosil P48 as fitted by computer simulations on spectral response data.

Al-gettering temperature	L_{diff} [µm]
ungettered	160
700	130
750	125
800	143
850	160
900	162
950	180
1000	170
1050	145

Table 3. Comparison of L_{diff} for ungettered reference cells and Al-gettered cells at the optimum temperature T_{opt} as determined by fitting of spectral response data.

Material	ungettered	gettered	
	L_{diff} [µm]	T_{opt} [°C]	L_{diff} [µm]
Baysix	110	850	105
Eurosolare P43	130	900	135
Eurosolare P48	160	950	180
Solarex	90	800	70
EMC	100	850	130
EFG	20	900	75
RGS	<20	700	20

HYDROGEN PASSIVATION STUDY

Apart from gettering techniques the passivation of crystal defects like grain boundaries and dislocations by hydrogen is a further option to improve the cell parameters. Different authors report on benefiting hydrogen treatments for EFG [7], RGS and Eurosil [8]. In our study we used a MIRHP (Microwave Induced Remote

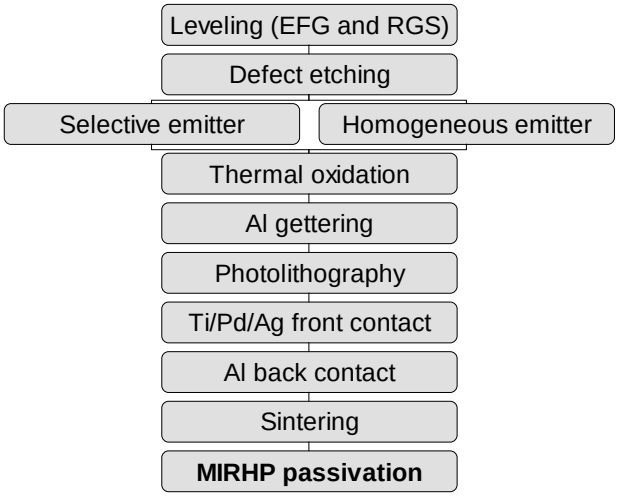

Fig. 3. Process sequence for the MIRHP passivation study

Hydrogen Plasma) passivation technique presented in [8]. For separating the benefit from Al-gettering and MIRHP passivation, our solar cell process was modified in a second study as shown in Fig. 3.
In order to compare the influence of a selective and a homogeneous emitter on the solar cell parameters during passivation, the samples were split and both emitter structures were processed. This time a thermal oxide was formed on the cell surface in order to be sure to just investigate the bulk passivation effect. We used the optimum Al-gettering temperature for each of the seven materials as obtained in the first study. The MIRHP passivation was carried out as the last step after cell metallization. In this way it was possible to characterize the Al-gettered cells prior to and after MIRHP passivation in order to get information about the improvement resulting from the hydrogen passivation step.

MIRHP passivation - Results

In the following results are presented which are all based on solar cells including a selective emitter structure unless otherwise stated. In Fig. 4 spectral response data for a Baysix solar cell before and after MIRHP passivation are shown. The absolute IQE is again fitted by computer simulations to extract L_{diff}. A large increase in L_{diff} after the passivation can be seen resulting in a gain in J_{sc} of 1.0 mA/cm^2.

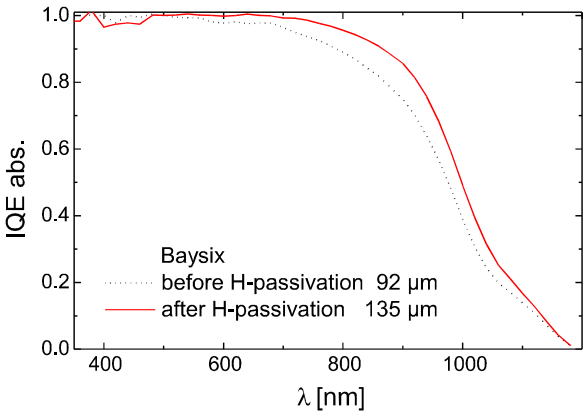

Fig. 4. Spectral response data for a Baysix solar cell before and after MIRHP passivation.

An even more dramatic effect was observed in the ribbon materials. Fig. 5 provides an example for an EFG solar cell before and after MIRHP passivation. An increase in L_{diff} of 83 µm has been observed which translates into a gain in J_{sc} of 3.8 mA/cm^2.
The aim of this study was to find the optimum passivation time for all materials, therefore we measured the cells every 30 minutes during passivation. The gain in efficiency for all materials can be seen in Fig. 6. Improvements in all cell parameters were observed for all materials and the efficiency η could be increased up to 30% relative in the case of the ribbon materials.

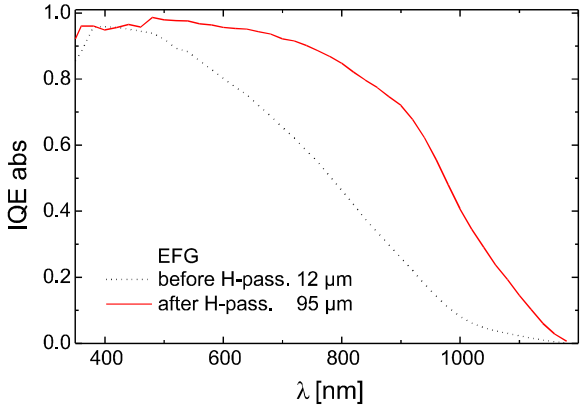

Fig. 5. Spectral response data for an EFG solar cell before and after MIRHP passivation.

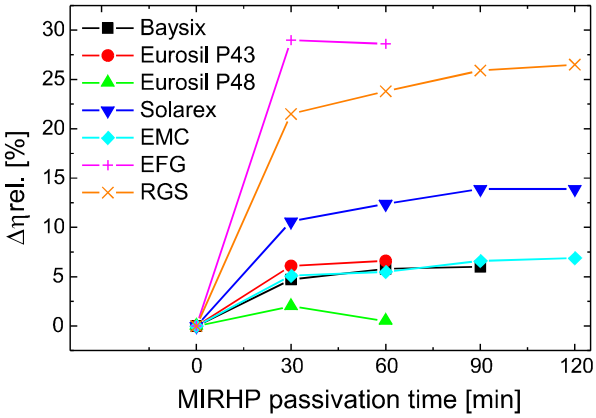

Fig. 6: Relative gain in efficiency for all used materials during MIRHP passivation.

A similar behavior was found for V_{oc}. We obtained an increase in V_{oc} of 35-40 mV for the ribbon Si materials, but also all the other materials showed a significant effect.
Up to now all presented results were obtained with the selective emitter structure. While we saw the same behavior of J_{sc} and V_{oc} during the MIRHP passivation when comparing the selective and the homogeneous emitter structure, a distinct difference in fill factor dependence was observed. Fig. 7 shows the change in fill factor during the passivation of the homogeneous emitter structure. During the first 30 minutes of the passivation we could see the same increase as for the selective emitter structure, but for longer passivation times a clear decrease has been found. This decrease which cannot be observed for the selective emitter structure in this distinctness causes a loss in efficiency for longer MIRHP passivation times. This is in agreement with former experiments [8,9].
In Table 4 the MIRHP passivation results are summarized. Given are the relative and absolute gains in efficiency $\Delta\eta_{rel}$ and $\Delta\eta_{abs}$ for the optimum MIRHP passivation time t_{opt}. We have improvements for all materials but again an especially good increase for the ribbon Si materials of nearly 30% relative.

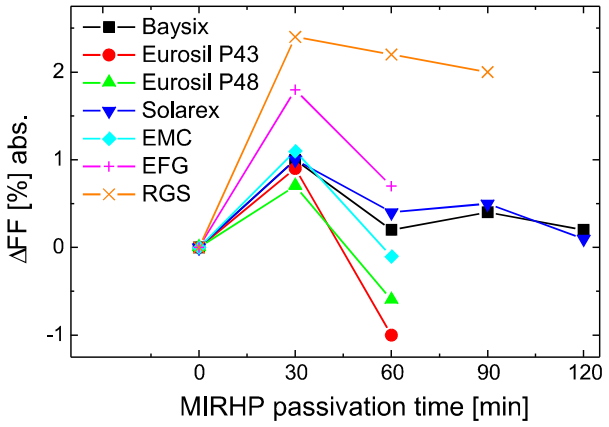

Fig. 7. Behavior of the fill factor during MIRHP passivation for the homogeneous emitter structure.

Table 4. Improvements in efficiency for all used materials at the optimum MIRHP passivation time t_{opt}.

Material	MIRHP Pass.	selective emitter	
	t_{opt} [min]	$\Delta\eta_{rel}$ [%]	$\Delta\eta_{abs}$ [%]
Baysix	90	6	0.6
Eurosil P43	30	7	0.6
Eurosil P48	30	2	0.2
Solarex	120	14	1.2
EMC	120	7	0.7
EFG	30	29	2.1
RGS	120	27	1.5

FUTURE PLANS

Our future activities will include the combination of an additional mechanical V-texturing step with the optimal Al-gettering temperature and the MIRHP hydrogen passivation. First results on Bayer RGS show an efficiency of 11.1% (including DARC). This is yet without using the optimal Al-gettering temperature, so we look forward to improve this result soon.

CONCLUSIONS

The behavior of seven cast mc and ribbon Si materials has been investigated in two studies. In the first Al-gettering study we found the optimum gettering temperature for all materials. While a decrease in L_{diff} was seen in Solarex material and no improvements found in Baysix and Eurosil P43, all other materials showed a marked increase. Especially the efficiency of the ribbon Si materials could be improved.
The second MIRHP hydrogen passivation study delivered the optimum passivation times for all materials. Improvements in all cell parameters for all materials could be observed. EFG and Bayer RGS showed the highest gains in efficiency of up to 30% relative. The homogeneous emitter structure gave the same results during the first 30 minutes of the passivation, but a significant decrease in fill factor was observed for longer passivation times.

ACKNOWLEDGEMENTS

We would like to thank M. Keil for technical assistance during solar cell processing. This work was supported by the German BMBF under contract number 0329557A and within the JOULE program of the European Commission under contract number JOR3-CT95-0030.

REFERENCES

[1] S. Narayanan, S. R. Wenham, M. A. Green, *Appl. Phys. Lett*. **48**, 1986, 873

[2] L. A. Verhoef, P.-P. Michiels, W. C. Sinke, C. M. M. Denisse, M. Hendriks, R. J. C. van Zollingen, *Appl. Phys. Lett*. **57**, 1990, 2704

[3] A. Rohatgi, S. Narasimha, S. Kamra, P. Doshi, C. P. Khattak, K. Emery, H. Field, *Proc. 25th IEEE PVSC*, 1996, 741

[4] J. P. Kalejs, *J. Crystal Growth* **128**, 1993, 298

[5] G. Hahn, M. Spiegel, S. Keller, A. Boueke, P. Fath, G. Willeke, E. Bucher, *Proc. 14th EC PVSEC*, 1997, in print

[6] C. Zechner, P. Fath, G. Willeke, E. Bucher, *Proc. 14th EC PVSEC*, 1997, in print

[7] P. Sana, A. Rohatgi, J. P. Kalejs, R. O. Bell, *Appl. Phys. Lett*. **64**, 1994, 97

[8] M. Spiegel, P. Fath, K. Peter, B. Buck, G. Willeke, E. Bucher, *Proc. 13th EC PVSEC*, 1995, 421

[9] M. Spiegel, S. Keller, P. Fath, G. Willeke, E. Bucher, *Proc. 14th EC PVSEC*, 1997, in print